

# Soil Backgrounds Impact Analysis on Chlorophyll Indices Using Field, Airborne and Satellite Hyperspectral Data

A. Bannari <sup>1</sup> and K. Staenz <sup>2</sup>

<sup>1</sup> *Remote Sensing and Geomatics of Environment Laboratory  
Department of Geography, University of Ottawa, Ottawa (Ontario), Canada K1N 6N5*

<sup>2</sup> *Alberta Terrestrial Imaging Center (ATIC)/ Department of Geography, University of  
Lethbridge, 400, 817 - 4th Avenue South, Lethbridge, Alberta, Canada T1J 0P3*

## Abstract

In precision agriculture, crop nitrogen status can be estimated based on the measurement of leaf chlorophyll content at specific stages of crop development. Over the last decade, several spectral chlorophyll indices have been developed to estimate chlorophyll content both at the leaf and the canopy level from different crop types using hyperspectral remote sensing data. For an accurate interpretation of chlorophyll indices derived from hyperspectral data, a “true” chlorophyll content value attributed only to the crop cover signal and free from any contribution of non-photosynthetic elements is required. However, in remote sensing, in spite of the correction and the standardization of the various radiometric distortions such as due to topography, atmosphere, sensor drift, and Bidirectional Reflectance Distribution Function (BRDF) effects, the chlorophyll indices remain sensitive up to a certain degree to the artifacts caused by the soil optical properties particularly in an earlier stage of crop growth. This chapter focuses on the evaluation and comparison of the sensitivity of several chlorophyll indices to bare soils optical property variations. In order to achieve the goal of this investigation, field spectroradiometric measurements were used as well as hyperspectral data acquired with the Probe-1 airborne and Hyperion Earth Observing -1 (EO-1) satellite sensors. The field-based reflectance measurements were acquired above 90 bare soil plots with various optical properties and selected from different agricultural lands. Probe-1 and Hyperion EO-1 data were acquired over the study site on June 28, 2000 and June 30, 2002, respectively. Imagery data were spectrally and radiometrically calibrated, as well as atmospherically corrected. After these pre-processing steps, sixty spectral signatures of different bare soils with various optical properties were extracted from each set of data for use in the analysis. The obtained results show an excellent agreement between the accuracies estimated from field, airborne and satellite data. Indices SIPI, PSSRa and MTCI show a very high root mean square error (RMSE) related to optical background variation. The indices SIPI, SRPI, NDPI, NPCI, GNDVI, CAI and HNDVI have a non-negligible RMSE related to the optical properties of bare soils, and will be very difficult to interpret at a low leaf area index (LAI). PSNDa, hNDVI and PRI show an RMSE less than 20%. The most insensitive

index of this group is the PRI with an RMSE less than 6 %. However, these errors remain significant. Independently from the data source and from the bare soil background, CARI, MCARI and TCARI indices are basically not sensitive to changes in soil optical properties with a RMSE less than 1.2 % and will permit a better estimation of chlorophyll content in sparse crop cover environment.

**Keywords:** chlorophyll indices, soil optical properties, precision agriculture, hyperspectral remote sensing, field spectroradiometric measurements, Probe-1 and Hyperion EO-1 sensors.

## 1. Introduction

Nitrogen concentration in crop cover is related to chlorophyll content and, therefore, indirectly to one of the basic plant physiological processes. When nitrogen supply surpasses the vegetation's nutritional needs, the excess is eliminated by runoff and water infiltration leading to pollution of aquatic ecosystems (Daughtry *et al.*, 2000; Wood *et al.*, 1993). This nitrogen loss to the environment represents an economic loss for farmers. However, inappropriate reduction of nitrogen supply could result in reduced yields and, subsequently, substantial economic losses. With this impasse, the optimal solution is an adequate assessment of the nitrogen status and its variability in agricultural landscapes. Since yield is determined by crop condition at the earlier stages of growth, it is mandatory to provide farmers with nitrogen status at those stages in order to supply appropriate rates based upon an accurate assessment of plant growth requirements and deficiencies (Haboudane *et al.*, 2002). For this purpose, remote sensing techniques have been used to assess crop conditions relative to nitrogen status and effects. Foliage spectral properties, reflectance and transmittance, were found to be affected by nitrogen deficiency (Blackmer *et al.*, 1996). Nitrogen shortage reduces leaf chlorophyll content and, therefore, increases its transmittance at visible wavelengths. Thus, reflected radiation from crop leaves and canopies has been used both to estimate chlorophyll content of crop canopies (Daughtry *et al.*, 2000; Filella *et al.*, 1995) and to assess nitrogen variability and stress (Blackmer *et al.*, 1994 and 1996). Over the last decade, several spectral chlorophyll indices have been developed to estimate chlorophyll content both at the leaf and at the canopy levels using hyperspectral remote sensing data of different crop types (Haboudane *et al.*, 2002; Blackburn, 1998a and 1998b; Chappelle *et al.*, 1992). Theoretically, the "ideal" chlorophyll index should be sensitive only to chlorophyll content in crop cover, but insensitive to soil background (colour, brightness, etc.), less sensitive to leaf area index (LAI) variations, independent of the spatial resolution of the sensors, and little affected by atmospheric and environmental effects, the drift of the sensor radiometric calibration, as well as solar illumination geometry and sensor viewing conditions, and not saturate rapidly. These effects intervene simultaneously during *in-situ* measurements and at the time of the airborne and/or satellite data acquisition. Consequently, it is impossible to design an index which is sensitive only to the desired variable and totally insensitive to all other parameters (Daughtry *et al.*, 2000; Bannari *et al.*, 1995; Kim *et al.*, 1994). However, in remote sensing, in spite of the correction and the standardization of the various radiometric distortions (topography, atmosphere, sensor drift, BRDF, etc.) chlorophyll indices remain always sensitive to the artifacts caused by soil optical properties particularly in an earlier stage of crop growth (sparse or fairly dense crop cover). Indeed, the effects of the underlying soil optical properties are very difficult to correct because not all soils are similar in the scene. Different soils have different spectral

reflectance behaviour because many factors influence the soil reflectance (Huete, 1989; Irons *et al.*, 1989). These are mineral composition, colour, brightness, moisture, organic matter content, salt and sodium content, roughness, and texture. In addition, size and shape of soil aggregates also influence the soil reflectance. These soil property variations affect the spectral response of soil and crop canopies and induce noise to the relationships between reflectance data and crop characteristics, such as LAI, absorbed photosynthetically active radiation (APAR), and chlorophyll content (Bannari *et al.*, 1996). These artifacts are likely to increase the chlorophyll index due to the spectral variations of the soils and not to an increase of the chlorophyll content. This chapter focuses on the evaluation and comparison of the sensitivity of several hyperspectral chlorophyll indices (PRI, NDPI, GNDVI, hNDVI, SIPI, SRPI, NPCI, PSSRa, PSNDa, MTCl, CAI, CARI, MCARI, and TCARI) to bare soils optical property variations using field spectroradiometric measurements as well as hyperspectral data acquired with the Probe-1 airborne and Hyperion EO-1 satellite hyperspectral sensors in the beginning of the growing season. With a sparse vegetation cover, the soil background becomes very important to consider using these indices

## 2. A Review of Spectral Chlorophyll Indices

Hyperspectral remote sensing is very often used to quantify plant photosynthetic pigment content. Plant pigments have a distinct spectral absorption characteristic, which means potential discrimination between them. Numerous studies and experiments have been undertaken in the search for spectral chlorophyll indices for accurate chlorophyll estimation at the leaf or the canopy level using hyperspectral remote sensing (i.e., laboratory and ground spectroradiometric measurements, model simulations and/or image data). Empirical approaches are based on simple relations established between chlorophyll content and spectral data, such as simple spectral analysis (Blackmer *et al.*, 1996; Mariotti *et al.*, 1996) and the analysis of the red-infrared spectral transition, the red-edge (Horler *et al.*, 1983; Guyot and Baret, 1988; Curran *et al.*, 1990 and 1991; Munden *et al.*, 1994; Pinar and Curran, 1996; Gitelson *et al.*, 1996; Filella and Peñuelas, 1994; Jago *et al.*, 1999; Zaroc-Tejada and Miller, 1999; Zarco-Tejada, 2000). In order to minimize the effects of soil background optical properties or the acquisition geometry (view/illumination) on the red-edge parameters, scientists have analyzed the potential of the first and second spectrum derivatives (Peñuelas *et al.*, 1994; Elvidge and Chen, 1995; Peñuelas and Filella, 1998; Jago *et al.*, 1999; Daughtry *et al.*, 2000; Gao, 2006). Other methods indicate that the logarithm of the inverse of the reflectance at specific wavelengths is well correlated with chlorophyll content (Peñuelas *et al.*, 1994; Balckburn, 1999). Semi-empirical approaches have a physical basis, but their mathematical formulation is related empirically to spectral data. In the literature, different indices for detecting and predicting chlorophyll status were developed (Baret *et al.*, 1988; Gamon *et al.*, 1992; Chappel *et al.*, 1992; Carter, 1994; Filella *et al.*, 1995; Jacquemoud *et al.*, 1996; Rollin and Milton, 1998; Blackburn, 1998a and 1998b; Haboudane *et al.*, 2002; Zhang *et al.*, 2008). A review of the spectral chlorophyll indices used in this chapter is given below, and their equations are presented in Table 1.

The *Photochemical Reflectance Index* (PRI) was developed to estimate the photosynthetic activity of canopies (Gamon *et al.*, 1992). It is a physiological reflectance index, which correlates (coefficient of determination  $R^2 > 0.91$ ) with the epoxidation state of the xanthophylls cycle pigments (i.e., a particular group of carotenoids, violaxanthin,

antheraxanthin, and zeaxanthin), and with the efficiency of the plant canopy's photosynthesis. The epoxidation state is the content of xanthophylls cycle pigments. This xanthophylls cycle may be associated with a diurnal reduction in photosynthetic efficiency (Gamon *et al.*, 1992). Therefore, the epoxidation state of the xanthophylls cycle pigments may be a useful indicator of short-term changes in photosynthetic activity. In several studies, this index showed its usefulness in the assessment of radiation use efficiency at the canopy-level. Filella *et al.* (1996) showed that PRI is significantly correlated ( $R^2 = 0.88$ ) with epoxidation, zeaxanthin, and photosynthetic radiation use efficiency for a cereal canopy. Penuelas *et al.* (1997) found significant results to assess photosynthetic radiation use efficiency at the leaf-level in Mediterranean trees, *Quercus ilux* and *Phillyrea latifolia*. Zarco-Tejada *et al.* (2005) showed that PRI is more sensitive to Chl-ab / carotenoid ratios ( $R^2 = 0.50$ ) than to Chl-ab alone ( $R^2 = 0.45$ ) or the carotenoid content for *Vitis vinifera* L ( $R^2 = 0.27$ ) leaves. The PRI was found not affected as much by changing viewing angles for wheat chlorophyll content prediction using the *Compact High Resolution Imaging Spectrometer* (CHRIS) on the platform *PRoject for On-Board Autonomy* (PROBA). This is because the PRI is in the visible part of the spectrum and, therefore, is not influenced by anisotropy in the near infrared. However, this index performs better for wheat chlorophyll content estimation at the canopy level (biomass per unit ground area) than for wheat chlorophyll contents per leaf (Oppelt and Mauser, 2007).

Spectral Chlorophyll Indices	Authors
$PRI = (r_{550} - r_{531}) / (r_{550} + r_{531})$	Gamon <i>et al.</i> (1992)
$SRPI = r_{430} / r_{680}$	Penuelas <i>et al.</i> (1993)
$NDPI = (r_{430} - r_{680}) / (r_{430} + r_{680})$	Penuelas <i>et al.</i> (1993)
$NPCI = (r_{680} - r_{430}) / (r_{680} + r_{430})$	Penuelas <i>et al.</i> (1994)
$SIPi = (r_{800} - r_{445}) / (r_{800} - r_{680})$	Penuelas <i>et al.</i> (1995)
$GNDVI = (r_{801} - r_{550}) / (r_{801} + r_{550})$	Gitelson <i>et al.</i> (1996)
$PSND_a = (r_{800} - r_{680}) / (r_{800} + r_{680})$	Blackburn (1998a)
$PSSR(a) = r_{800} / r_{680}$	Blackburn (1998a)
$CARI = [(r_{700} - r_{670}) - 0.2 * (r_{700} - r_{550})]$	Kim <i>et al.</i> (1994)
$MCARI = [(r_{700} - r_{670}) - 0.2 * (r_{700} - r_{550})] * (r_{700} / r_{670})$	Daughtry <i>et al.</i> (2000)
$TCARI = 3 * [(r_{700} - r_{670}) - 0.2 * (r_{700} - r_{550}) * (r_{700} / r_{670})]$	Haboudane <i>et al.</i> (2002)
$CAI = \int_{r_{600}}^{r_{735}} r_{EQ} dx, \quad \text{where} \quad r_{EQ} = r_{Sc} / r_{ec} \cdot$	Oppelt & Mauser (2001)
where $r_{Sc}$ is the reflectance of the vegetation spectrum at band c, $r_{ec}$ is the reflectance of the envelope at band c, and $r_{EQ}$ is the envelope quotient (see Oppelt and Mauser (2001 and 2004) for provision of more details about this index and for the calculation and extraction of all these parameters).	
$HNDVI = (R_{827} - R_{668}) / (R_{827} + R_{668})$	Oppelt & Mauser (2004)
$MTCI = (r_{753.75} - r_{708.75}) / (r_{708.75} - r_{681.25})$	Dash and Curran (2004)

Table 1. Equations of chlorophyll indices ( $r_\lambda$  indicates the reflectance in a band centered at a specific wavelength  $\lambda$ ).

The *Simple Ratio Pigment Index* (SRPI) based on the ratio of the carotenoid and Chl-a content was proposed by Penuelas *et al.* (1993). Penuelas *et al.* (1993 and 1994) found that SRPI correlates well ( $R^2 > 0.95$ ) with different levels of mite attacks in apple trees, as the carotenoid / Chl-a ratio increases with increasing level of mite attack. Similar performances were observed for the same ratio from a wide range of leaves from different species (maize, wheat, tomato, soybean, sunflower, sugar beet, and maple) when the SRPI was highly correlated ( $R^2 > 0.95$ ) with carotenoid / Chl-a ratio (Penuelas *et al.*, 1995). The SRPI was found to be slightly sensitive to low chlorophyll content ( $< 50 \text{ mg} / \text{cm}^2$ ). Penuelas *et al.* (1995) also demonstrated that this index is very sensitive to the leaf structure.

The *Normalized Difference Pigment Index* (NDPI) was proposed by Penuelas *et al.* (1993) in the same way as SRPI to evaluate the ratio of total pigments to Chl-a. Penuelas *et al.* (1993, 1994 and 1995) found that in maize, wheat, tomato, soybean, sunflower, sugar beet, maple, and aquatic plants the NDPI was highly correlated ( $R^2 \geq 0.91$ ) with the ratio of total carotenoids and Chl-a measured at the leaf and plant levels. This index was found sensitive to the leaf surface and structure (Araus *et al.*, 2001). For wheat chlorophyll content estimation in intermediate stage development (approximately 70% of the fields were covered by wheat crop) using the Hyperion EO-1 data against those derived from the SPAD-502 measurements and chemical laboratory analysis, the NDPI showed satisfactory results with an index of agreement of 0.66 and a root mean square error (RMSE) of  $2.89 \text{ } \mu\text{g} / \text{cm}^2$  (Bannari *et al.*, 2008).

In a study related to nitrogen (N) and water in sunflower leaves, Penuelas *et al.* (1994) proposed the *Normalized Pigment Chlorophyll Ratio Index* (NPCI). This index varies with total pigment and chlorophyll content and is associated with plant physiological state. This index is sensitive to the proportion of total photosynthetic pigments to chlorophyll, particularly applicable to N stress (Penuelas *et al.*, 1994). For wheat crop (*Triticum aestivum* L.), NPCI was significantly correlated ( $R^2 = 0.84$ ) with total chlorophyll content using field-based reflectance measurements (Riedell and Blackmer, 1999). Exploring a wide range of hyperspectral chlorophyll indices, laboratory based-reflectance data and wheat leaf chlorophyll content estimated from chemical laboratory analysis, Bannari *et al.* (2007a) found that NPCI is significantly correlated ( $R^2 = 0.84$ ) with Chl-ab / Chl-a ratio than with the Chl-ab content only.

Considering a wide range of leaves from several species (corn, wheat, tomato, soybean and sunflower) with the aim of assessing the pigment ratio, Penuelas *et al.* (1995) proposed the *Structure Insensitive Pigment Index* (SIPI). They established an empirical estimation of the carotenoid / Chl-a ratio and found that SIPI provided the best estimate for a range of individual leaves of different species (maize, wheat, tomato, soybean, sunflower, sugar beet, and maple) and conditions ( $R^2 \geq 0.95$ ). Blackburn (1998a) confirmed that this index has a curvilinear relationship with the carotenoid / Chl-a ratio, which is best described using a logarithmic model (i.e., this model gives the highest coefficient of determination:  $R^2 = 0.86$ ). The SIPI lacks sensitivity for low values of the carotenoid / Chl-a ratio and becomes more sensitive for higher values. Using physical simulation on *Vitis vinifera* L. leaves, Zarco-Tejada *et al.* (2005) demonstrated that SIPI is more sensitive to carotenoids and Chl-ab / carotenoid ratio than to chlorophyll Chl-ab content alone.

The *Green Normalized Difference Vegetation Index* (GNDVI) was developed by Gitelson *et al.* (1996) using a green band in a study related to the remote sensing of global vegetation and EOS-MODIS (*Earth Observing System - Moderate Resolution Imaging Spectroradiometer*) data. The development of the GNDVI is based on the idea that an index for chlorophyll estimation should be invariant with respect to pigments other than chlorophyll and should not be influenced by factors including background and atmosphere. Blackburn (1999) reported that there is a curvilinear relationship between GNDVI and the total chlorophyll content ( $R^2 = 0.82$ ). He used this index in a laboratory experiment using stacks of leaves, obtained from four species of deciduous trees at various stages of senescence. He observed that over the wide range of chlorophyll contents, which can be experienced at the canopy scale, GNDVI was found to be sensitive to low content ( $\sim 500 \text{ mg / cm}^2$ ) only. The use of reflectance in a narrow green band,  $r_{550}$ , rather than  $r_{Green}$  (reflectance in the range of 540-570 nm) in the formulation of this index did not improve the relationship with total chlorophyll content. In addition, no relationship was found between GNDVI and matorral vegetation canopy chlorophyll content per unit ground area (Blackburn, 1999).

The *Pigment Specific Simple Ratio* (PSSR) was proposed by Blackburn (1998a) for the estimation of Chl-a (PSSR<sub>a</sub>), Chl-b (PSSR<sub>b</sub>), and carotenoids (PSSR<sub>c</sub>) contents at the leaf level using samples from deciduous trees at various stages of senescence. Blackburn (1998b) found that PSSR<sub>a</sub> has a strong relationship with Chl-a ( $R^2 = 0.97$ ), and McNairn *et al.* (2001) reported the same conclusion for Chl-a estimation in corn and beans. However, the PSSR<sub>c</sub> failed to predict carotenoid content in individual leaves of four deciduous tree species at various stages of senescence (Blackburn, 1998b). In another experiment on matorral vegetation canopy, Blackburn and Steele (1999) reported a reasonably linear relationship between PSSR<sub>a</sub> and Chl-a content per unit ground area ( $R^2 = 0.71$ ). However, the relationship was much weaker for low Chl-a contents (0 to  $500 \text{ mg / cm}^2$ ). Lower linear relationships were also found between PSSR<sub>b</sub> and Chl-b ( $R^2 = 0.68$ ) and PSSR<sub>c</sub> and carotenoid ( $R^2 = 0.50$ ) content per unit ground area. In this study, only the PSSR<sub>a</sub> was considered.

Blackburn (1998a) also developed the *Pigment Specific Normalized Difference* (PSND) index to estimate individual pigment Chl-a (PSND<sub>a</sub>), Chl-b (PSND<sub>b</sub>), and carotenoid (PSND<sub>c</sub>) contents. Like the PSSR indices, the PSND<sub>a</sub> and PSND<sub>b</sub> were found to have a strong exponential relationship with Chl-a and Chl-b ( $R^2 > 0.91$ ), respectively. However, PSND<sub>c</sub> failed to predict carotenoid content in individual leaves of four deciduous tree species at various stages of senescence (Blackburn, 1998b). Blackburn and Steele (1999) found a lower correlation ( $R^2 < 0.51$ ) between these indices and the pigment contents of matorral vegetation canopies per unit ground area than in his previous studies (Blackburn, 1998a and b). The author suggested that this is due to variable background conditions and the structural/spectral complexity of the study sites. As for the PSSR<sub>a</sub>, only the PSND<sub>a</sub> is used in this study.

The *Chlorophyll Absorption in Reflectance Index* (CARI) was developed by Kim *et al.* (1994) and was designed to reduce the variability of photosynthetically active radiance due to the presence of diverse non-photosynthetic materials. Due to the sensitivity of CARI to soil background, Daughtry *et al.* (2000) presented the *Modified Chlorophyll Absorption in*

*Reflectance Index* (MCARI). The main change from CARI is the introduction of the ratio ( $r_{700} / r_{670}$ ) to minimize the combined effect of the underlying soil reflectance and the canopy non-photosynthetic materials. Even though this index was developed to be both responsive to chlorophyll variations and resistant to non-photosynthetic material effects, Daughtry *et al.* (2000) reported that the MCARI is still influenced by the optical properties of the soil background. In order to minimize the underlying soil contribution, they suggested that the MCARI be normalized with a soil line vegetation index like the *Optimized Soil-Adjusted Vegetation Index* (OSAVI; Rondeaux *et al.*, 1996). Combining these spectral indices will further reduce the background contributions and enhance the sensitivity to leaf chlorophyll content variability at the same time. Daughtry *et al.* (2000) found that the MCARI / OSAVI ratio was linearly related to leaf chlorophyll contents ( $R^2 = 0.87$ ) over a wide range of foliage cover of corn (*Zea mays* L.) and soil backgrounds. The combined use of the spectral indices MCARI and OSAVI was successful in producing an accurate assessment of crop chlorophyll contents from remote sensing data (Daughtry *et al.*, 2000). However, this normalization combination was not implemented for predictive purposes, nor have further developments dealt with LAI effects on pigment content estimation from canopy reflectance measurements. In addition, Haboudane *et al.* (2002) noted the limited sensitivity of MCARI for low pigment contents ( $> 5 \mu\text{g} / \text{cm}^2$ ).

Haboudane *et al.* (2002) presented another variation of the MCARI, the *Transformed Chlorophyll Absorption in Reflectance Index* (TCARI). The main reason for developing TCARI was to improve sensitivity for low chlorophyll values of corn. However, according to these authors, this index is sensitive to the underlying soil properties, particularly for low LAIs ( $< 2.5$ ). In the same study of integrated narrow-band indices for corn-crop chlorophyll prediction, Haboudane *et al.* (2002) proposed the TCARI / OSAVI ratio. The use of this ratio enabled accurate prediction of corn chlorophyll content from hyperspectral remote sensing imagery. These authors established a scaling-up relationship to make chlorophyll estimations as a function of the TCARI / OSAVI ratio derived from above canopy reflectance using *Compact Airborne Spectrographic Imager* (CASI) data. The ratio was found to be relatively insensitive to canopy cover variations, even for very low LAIs ( $< 1.5$ ). The best fits were obtained for a logarithmic and polynomial function with  $R^2$  values exceeding 0.98. Zarco-Tejada *et al.* (2005) showed that the TCARI / OSAVI was successfully correlated with the Chl-ab content at the canopy scale of *Vitis vinifera* L. using *Reflective Optics Spectrometric Imaging System* (ROSIS) and CASI data ( $R^2 = 0.67$ ). Huang *et al.* (2004) found a significant logarithmic relationship ( $R^2 = 0.78$ ) between TCARI / OSAVI derived from field reflectance measurements and wheat chlorophyll arbitrary values measured with the SPAD (Soil-Plant Analyses Development)-502 meter. Exploring CHRIS-PROBA data for wheat crop chlorophyll content prediction in shaded and sunlit portions of the field, Oppelt and Mauser (2007) showed that using the off-forward-looking angle ( $+ 36^\circ$  from the nadir) chlorophyll content per leaf area is weakly correlated with TCARI / OSAVI ( $R^2 = 0.56$  and  $R^2 = 0.49$  for the sunlit and shaded sides, respectively). However, this index showed a relatively high correlation ( $R^2 = 0.71$ ) with chlorophyll content per biomass of the sunlit portion in the nadir viewing direction. They concluded that the TCARI / OSAVI ratio is significantly sensitive to the viewing angle geometry. In another study for the Chl-ab content estimation at the canopy scale of *Vitis vinifera* L. using CASI reflectance spectra, Meggio *et al.* (2008) demonstrated that BRDF effects significantly affect the TCARI / OSAVI ratio. According to

Wu *et al.* (2008), if different disturbances sources such as shadow, soil background, and non-photosynthetic materials, were considered, the integrated indices TCARI / OSAVI and MCARI / OSAVI are appropriate for chlorophyll estimation of different types of corns with high  $R^2$  of 0.88 and 0.94, respectively. In addition, these authors indicated that these two indices could be used to estimate the chlorophyll of wheat using Hyperion data ( $R^2$  of 0.68 and 0.76 for TCARI / OSAVI and MCARI / OSAVI, respectively). However, Kneubühler (2002) and Bannari *et al.* (2007 and 2008) showed that these indices, developed specifically for corn, performed poorly at the wheat canopy-level using Hyperion hyperspectral data. As well, Haboudane *et al.* (2008), the developer of the TCARI / OSAVI ratio, found that this ratio seems to be a good estimator of leaf chlorophyll content for corn canopies using CASI hyperspectral reflectance data ( $R^2 = 0.73$ ), but weak for wheat chlorophyll content estimation ( $R^2 = 0.29$ ).

The *Normalized Difference Vegetation Index* (NDVI) was proposed by Rouse *et al.* (1974) and was used in various regional and global applications for studying the state of vegetation using multispectral remote sensing (Bannari *et al.*, 1995). When hyperspectral data are used, the name of this index becomes the *Hyperspectral Normalized Difference Vegetation Index* (HNDVI). Oppelt and Mauser (2004) used the HNDVI in a study for monitoring physiological parameters of wheat. They found that HNDVI and OSAVI become insensitive at chlorophyll contents below 0.3 g/m<sup>2</sup> as well as above 1.5 g/m<sup>2</sup>. Nevertheless, it important to mention that these indices were developed for biomass and yield estimation, but not for chlorophyll content prediction.

The *Chlorophyll Absorption Integral* (CAI) was proposed by Oppelt and Mauser (2001) for chlorophyll content of maize (*Zea mays*) derived from *Airborne Visible/near-infrared Imaging Spectrometer* (AVIS) data. This index involves the position of the red edge as well as the depth of chlorophyll absorption at 680 nm (Chl-a) and 650 nm (Chl-b). According to these authors, CAI shows a very good correlation with the maize chlorophyll content per unit area or per unit mass ( $R^2 \geq 0.92$ ), and it could be a good predictor of wheat canopy chlorophyll content provided the dependence of the chlorophyll level on the wheat crop variety is taken into consideration. Oppelt and Mauser (2007) demonstrated that the CAI is the appropriate index to assess the chlorophyll content of both sunlit and shaded layers of wheat canopies using the data acquired with multi-angle CHRIS-PROBA sensor. However, even if the CAI was recommended for wheat crop chlorophyll content prediction (Oppelt and Mauser, 2004 and 2007), this index provide very poor results for wheat using Hyperion EO-1 data (Bannari *et al.*, 2008). Oppelt and Mauser (2001 and 2004) and Khurshid (2004) provide more details on the calculation and extraction of this index.

Using a ratio of the difference in reflectance between bands 10 and 9 and the difference in reflectance between bands 9 and 8 of the *Medium Resolution Imaging Spectrometer* (MERIS), Dash and Curran (2004) developed the *MERIS Terrestrial Chlorophyll Index* (MTCI). This index is used by the European Space Agency to produce the land surface biomass, a MERIS level-2 product. Due to its moderate spatial resolution (300 m x 300 m) and three-day re-visit time, MERIS is a potentially valuable sensor for the measurement and monitoring of terrestrial environment at regional to global scales (Verstraete *et al.*, 1999). However, using laboratory reflectance measurements for wheat crop chlorophyll content estimation, Bannari



*et al.* (2007a) showed that it would be very difficult or impossible to interpret the MTCI values at low LAI in the precision agriculture context. Additionally, Haboudane *et al.* (2008) found that this index is very sensitive to the LAI, predicting a weak correlation with wheat chlorophyll content ( $R^2 = 0.35$ ), but a higher one with corn chlorophyll ( $R^2 = 0.81$ ) using CASI airborne data.

### 3. Material and Methods

#### 3.1. Study Site and field data collection

The field, airborne and satellite data were collected in an agricultural region near Indian Head (50°N, 104°W), approximately 70 km east of Regina, Saskatchewan, Canada. The principal economic activities in this area are based on agriculture. Major crops grown are wheat, pea, canola and corn. This region was used in the context of a large project to investigate the potential of hyperspectral remote sensing in precision agriculture. In this project, the laboratory and the field measurements, and airborne and satellite hyperspectral data were investigated for plant water content estimation (Champagne *et al.*, 2003), nitrogen stress detection (Karimi *et al.*, 2005a and 2005b), LAI modelling and percent crop cover type mapping (Pacheco *et al.*, 2001, 2002, and 2008), crop residues estimation (Bannari *et al.*, 2006 and 2007b), and chlorophyll content prediction (McNairn *et al.*, 2001; Bannari *et al.*, 2007a and 2008).

The soils in the Indian Head and Regina regions are developed on lacustrine, alluvial lacustrine, alluvial glacio-fluvial, and glacial till parent materials in the brown, dark-brown, and black soil zone (Thie, 2006). Dark-brown chernozemic soils, which are the most productive of this group, occupy approximately 75% of the area. Thin black chernozemic soils (about 15 %) are developed on moderately fine and fine textured lacustrine parent materials. The brown soils (less than 2 %) are characterized by moderate-fine texture, and are generally rated as soils whereas the moderately coarse and coarse deposits. Gleysolic soils are generally most widely distributed, but are less represented in the study area. Azonal soils characteristic of the alluvium and hillwash complexer (about 10 %) occur in association with the main drainage channels or their adjacent floodplains. The objective of this study is not the characterization of each soil class using hyperspectral remote sensing, but the evaluation and comparison of the sensitivity of several chlorophyll indices to bare soils optical property variations. In order to achieve the goal of this investigation, different soils were selected based on the spatial representativeness of the major soil types from different agricultural lands with various optical and physico-chemical properties (colour, brightness, roughness, moisture, mineralogical composition, etc.). In the field, samples were taken from the soils upper layer (5 cm depth). Observations and remarks about each sample were noted and photographed using a 35 mm digital camera equipped with a 28 mm lens.

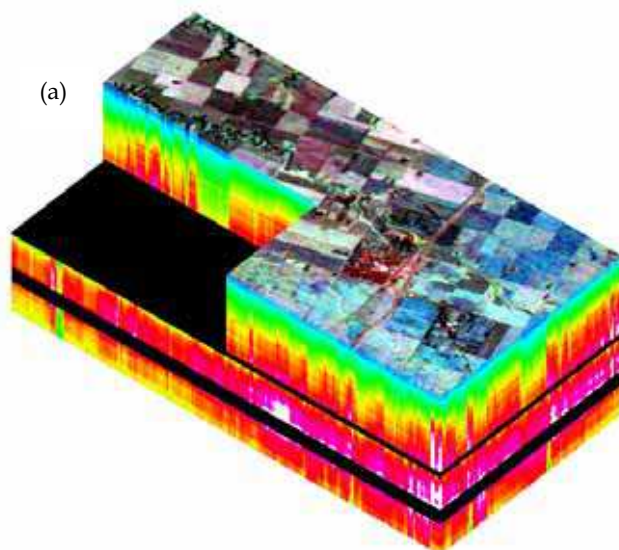
#### 3.2. Hyperion data acquisition

Satellite hyperspectral data were acquired on June 30, 2002 using the Hyperion hyperspectral sensor on NASA's Earth Observer-1 (EO-1) platform over the Indian Head site (Figure 1a). The launch of the Hyperion sensor in November 2000 marked the first operational test of a space-borne hyperspectral sensor covering both the visible and near-infrared (VNIR) and the short-wave infrared (SWIR) spectral regions (Beck, 2003). This

sensor is a pushbroom imaging spectrometer that acquires data in the along-track direction. It collects the upwelling radiance in 242 spectral bands, each approximately 10 nm wide at full width half maximum (FWHM) with an average spectral sampling interval of 10 nm. Hyperion has a single telescope and consists of two spectrographs, one covering the VNIR wavelengths range from 357 to 1055 nm, the other, the SWIR from 851 to 2576 nm. Since Hyperion is a pushbroom sensor, the entire swath is obtained in a single frame with a ground sampling distance of 30 m. Its telescope images the Earth onto a slit with a field-of-view (FOV) of  $0.624^\circ$ , resulting in a swath width of 7.65 km from a 705 km altitude. Each data set acquired by this sensor covers a nominal along-track length of 40 km. Figure 1a illustrates the 3D cube of the used Hyperion EO-1 data.

### 3.3. Probe-1 data acquisition

The airborne hyperspectral data were acquired using the Probe-1 sensor (Earth Search Sciences Inc., 2001) on Jun 28, 2000 over the Indian Head site (Figure 1b). The Probe-1 is a "whiskbroom style" instrument that collects data in cross-track direction by mechanical scanning and in along-track direction by movement of the airborne platform. This sensor acquires up-welling radiance in 128 bands in the 400 to 2500 nm wavelengths region. The at-sensor radiance is dispersed by four spectrographs onto four linear detector arrays with 32 bands each. This sensor covers the wavelength range continuously with small gaps in the strong 1380 nm and 1870 nm atmospheric water vapor absorption regions. The bandwidth is between 11 and 18 nm at FWHM. Probe-1 was mounted on a three-axis gyrostabilizer to minimize geometric distortion from the aircraft movement. The flying altitude was 2500 m above ground for a swath width of 3 km and a spatial resolution of 5 m at nadir. A non-differential GPS was recording the location of the aircraft during the flight. Figure 1b shows the 3D cube of the used Probe-1 airborne hyperspectral data.



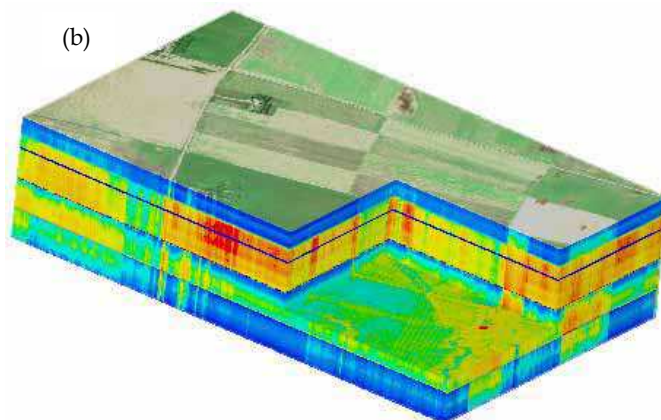


Fig. 1. Hyperspectral Hyperion EO-1 (a) and Probe-1 (b) 3D cubes.

### 3.4. Field spectroradiometric measurements

In order to achieve the goal of this investigation, spectroradiometric measurements were acquired above 90 bare soil plots selected from different agricultural lands with various optical and physicochemical properties (colour, brightness, roughness, moisture, mineralogical composition, etc.) using an ASD (*Analytical Spectral Devices*) spectroradiometer (ASD Inc., 1999). This instrument is equipped with two detectors operating in the VNIR and SWIR, between 350 and 2500 nm. It acquires a continuous spectrum with a 1.4 nm sampling interval from 350 to 1000 nm and a 2 nm one from 1000 to 2500 nm. The ASD resamples the measurements in 1-nm intervals, which allows the acquisition of 2151 contiguous bands per spectrum. The sensor is characterized by the programming capacity of the integration time, which allows a satisfactory signal-to-noise ratio as well as a great stability (ASD Inc., 1999).

Measurements were taken in the laboratory using two halogen lamps of 500 W each, equipped with an electrical current regulator. The data were acquired at nadir with a FOV of 25° and a solar zenith angle of approximately 5° by averaging twenty-five measurements. The spectroradiometer was installed on a tripod with a height of approximately 30 cm over the target, which makes it possible to observe a surface of approximately 177 cm<sup>2</sup>. A laser beam was used to locate the center of the ASD FOV. The reflectance factor of each soil sample was calculated by rationing target radiance to the radiance obtained from a calibrated "Spectralon panel" in accordance with the method described in Jackson *et al.* (1980). Corrections were made for the wavelength dependence and non-lambertian behavior of the panel. Only the VNIR wavelengths from 430 to 850 nm were required to calculate the chlorophyll indices used in this study (Table 1). The specific and requested wavelength ranges for each chlorophyll index were used from these measurements. Figure 2 shows the reflectance of the soil samples.

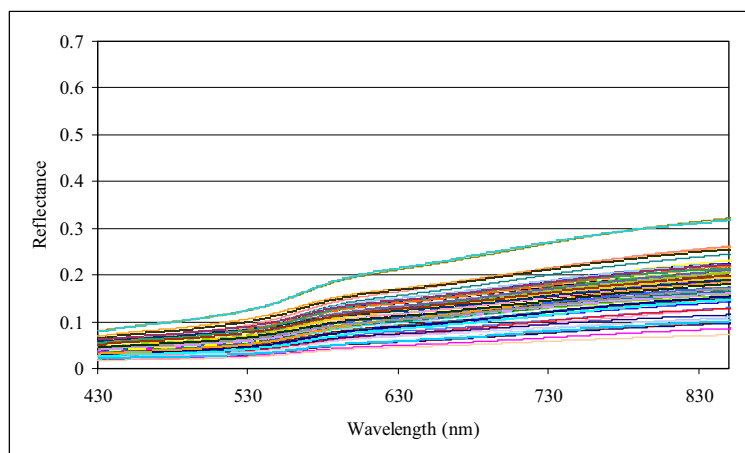


Fig. 2. Spectral signature of soils sampled at the field and measured in the lab using ASD.

### 3.5. Hyperion and Probe-1 data pre-processing

#### 3.5.1. Hyperion radiometric and spectral calibration

Hyperion EO-1 hyperspectral data were pre-processed with an aim to correct for sensor artifacts and atmospheric and geometric effects (Khurshid *et al.*, 2006). The *Imaging Spectrometer Data Analysis System* (ISDAS) developed at the *Canada Centre for Remote Sensing* (Staez *et al.*, 1998) was used to perform all the pre-processing steps. The procedure begins with geometric corrections (shift and rotation) of the SWIR data to spatially register them to the VNIR data. In fact, the SWIR data were corrected for a single pixel offset from pixels 129 to 256 across-track and rotated by  $0.22^\circ$ . Furthermore, the striping problem due to systematic noise caused by factors such as detector non-linearity, movement of the slit with respect to the focal plane and temperature effects (Kruse *et al.*, 2003) was corrected. In addition, the column dropouts caused by dead pixels (a dead pixel is a functional failure of a single detector element during acquisition) were then removed from the whole image cube (Sun *et al.*, 2008). This was followed by noise reduction using recently developed automated software tools (Khurshid *et al.*, 2006). To achieve this step, the raw imagery (digital numbers) recorded by the sensor was converted to radiance using the radiometric calibration coefficients (gains and offsets) derived in the laboratory and provided by NASA.

The data cube was subsequently analyzed to characterize the distortions of keystone and spectral smile (Neville *et al.*, 2004 and 2008). At this step, the data were cropped to exclude noisy bands resulting in a final data set that spans the spectral range from 426.82 to 2355.20 nm with a total of 192 bands, excluding the overlap bands between the VNIR and SWIR spectrographs. Keystone is a term used in hyperspectral remote sensing to refer to the inter-band spatial mis-registration in imaging spectrometers (Neville *et al.*, 2004). These distortions may be caused by geometric distortions or by chromatic aberration, or a combination of both. Due to these distortions, a particular spatial pixel, corresponding to a specific detector element in the across-track dimension, in one specific band, will not be registered on the ground with the corresponding pixel in the other spectral bands. Neville *et*

*al.* (2004) reported that the Hyperion sensor has keystone distortions, ranging from - 0.05 to 0.49 pixels for the VNIR spectrometer and - 0.06 to 0.07 pixels for the SWIR spectrometer. For our data, the keystone distortion varied from a minimum of - 0.075 pixels to a maximum of 0.3 pixels for the VNIR and - 0.075 to 0.1 pixels for the SWIR (Khurshid *et al.*, 2006). No keystone corrections were performed due to the lack of an appropriate resampling procedure providing sufficient geometric accuracy without minimal increase in noise.

Furthermore, the spectral smile/frown is a wavelength shift, which is a function of the across-track pixel (column) in the swath (Neville *et al.*, 2008). In an ideal case, all pixels in the across-track dimension correspond to the same wavelength. This wavelength shift is due to many sources, such as spatial distortions caused by the dispersion element, prism or grating, or by aberrations in the collimator and imaging optics (Neville *et al.*, 2008). To achieve spectral calibration, the radiance spectra were analyzed to evaluate the bandwidth and band's center position using five known atmospheric absorption features: 760 nm (oxygen), 940 nm and 1130 nm (water vapor), and 2005 nm and 2055 nm (carbon dioxide). The correct band center wavelengths and bandwidths are determined by correlating the at-sensor Hyperion radiance with a modeled at-sensor radiance calculated with the radiative transfer (RT) code MODTRAN 4.2 (Berk *et al.*, 1999). Wavelength shifts of 1 to 3 nm in the VNIR and SWIR were detected and applied after the atmospheric correction process.

### **3.5.2. Probe-1 radiometric and spectral calibration**

A laboratory calibration was completed for the Probe-1 sensor in April 2000 to obtain the dark current signal, radiometric coefficients, and to ascertain the center position of the spectral bands. However, a vicarious calibration of the sensor was required to correct for errors in gains and band centers, which resulted from the stresses experienced during transportation, installation and operation between the laboratory calibration and the over-flight (Secker *et al.*, 2001). This is an absolute calibration method, which produces a new set of gains that can be used to replace those derived in the laboratory.

To achieve spectral calibration of the Probe-1 data, the raw spectrum (digital numbers) recorded by the sensor was converted to radiance using the radiometric gains and offsets derived in the laboratory. As for the Hyperion data, the derived reflectance spectra were then analyzed to evaluate the band's center positions using five known atmospheric absorption features located at 760 nm (oxygen), 940 nm and 1130 nm (water vapor) and 2005 nm and 2055 nm (carbon dioxide). Wavelength shifts were then calculated, which best corrected the surface reflectance to obtain a smooth spectrum in the regions of these absorption features. These shifts were then applied to the Probe-1 data. The reflectance-based vicarious calibration was then applied in a next step to the data using the reflectance of an asphalt reference target acquired on the ground with an ASD spectroradiometer (Secker *et al.*, 2001). This site was then visually located in the Probe-1 imagery and an average spectrum was extracted for the calibration target. The spectrum from this target was then matched to the averaged ASD spectra of the same site. The differences between the two spectra were calculated and the Probe-1 radiometric coefficients were then adjusted to minimize the absolute reflectance difference until an error threshold was reached, which was set to 0.02 %. This process was carried out in ISDAS (Staenz *et al.*, 1998) with an iterative

numerical technique which provided a new set of optimal gains. These new gains were then applied to the raw digital numbers to calculate at-sensor radiance for the dataset.

### 3.5.3. Hyperion and Probe-1 surface reflectance retrieval

The calibrated at-sensor radiance data were converted to surface reflectance using a look-up table (LUT) approach to correct for the atmospheric effects (Staez and Williams, 1997). Two five-dimensional raw LUTs, each one for a 5% and 60% spectrally flat reflectance, with tunable breakpoints were generated with the MODTRAN 4.2 RT code to provide additive and multiplicative coefficients for the removal of atmospheric scattering and absorption effects. For this purpose, the midlatitude-summer atmosphere model and a continental-rural aerosol model was used. The input parameters for the RT code for Hyperion and Probe-1 data are presented in Table 2. The initial LUTs were then convolved with the Hyperion and Probe-1 spectral sensor characteristics and used in combination with a curve-fitting technique in the 940 and 1130 nm water vapor absorption regions to estimate the atmospheric water vapour content from the datasets themselves on a pixel-by-pixel basis (Green *et al.*, 1991; Gao and Goetz, 1990). The column atmospheric water vapour estimates are then used to interpolate the LUTs to retrieve surface reflectance. Subsequently, the reflectance data were corrected for smile effects.

Input Parameters/Dataset	Probe-1 data	Hyperion data
Date of over flight	June 28, 2000	June 30, 2002
Time of over flight (GMT)	17:10:00	17:36:00
Aircraft heading	110°	N/A
Sensor altitude (above sea level)	3.079 km	705 km
Terrain elevation (above sea level)	579 m	579 m
Solar zenith angle	34.35°	31.72°
Solar azimuth angle	132.55°	142.17°
Atmospheric model	Mid-latitude Summer	Mid-latitude Summer
Aerosol model	Continental (rural)	Continental (rural)
Water vapour content	1.5 g/cm <sup>2</sup>	1.5-2.5 g/cm <sup>2</sup>
Ozone column (as per model)	0.319 cm-atm	0.319 cm-atm
CO <sub>2</sub> mixing ratio (as per model)	357.5 ppm	365.00 ppm
Horizontal visibility	50 km	23 km

GMT= Greenwich Mean Time; ASL= Above Sea Level; ppm=parts per million

Table 2. Input parameters for the MODTRAN 4.2 radiative transfer code for Probe-1 data and Hyperion data.

Finally, the post-processing concluded the corrections by removing residuals that still remained after the correction of sensor artifacts and atmospheric effects. This step involves the calculation of correction gains and offsets using a spectrally flat target pixel approach (Staez *et al.*, 1999). The technique assumes that there are a number of pixels whose reflectance spectra are flat or nearly flat (feature-less), and their brightness range covers a major portion of the full range for all the pixels in the scene. A second-order polynomial fit to the reflectance spectra using  $\chi$ -squared as a goodness of fit measure is calculated on a pixel-by-pixel basis. The pixels with the smallest  $\chi$ -squared values are selected as "spectrally

flat target pixels". Finally, linear fits are performed on a band-by-band basis providing slopes and offsets, which are used as gain and offset for the correction of residual errors in the reflectance data.

After all these pre-processing steps, 60 spectral signatures representing different bare soils with various optical properties were extracted from bare soil of different agricultural fields from the Hyperion and Probe-1 imagery for the analysis (Figures 3 and 4).

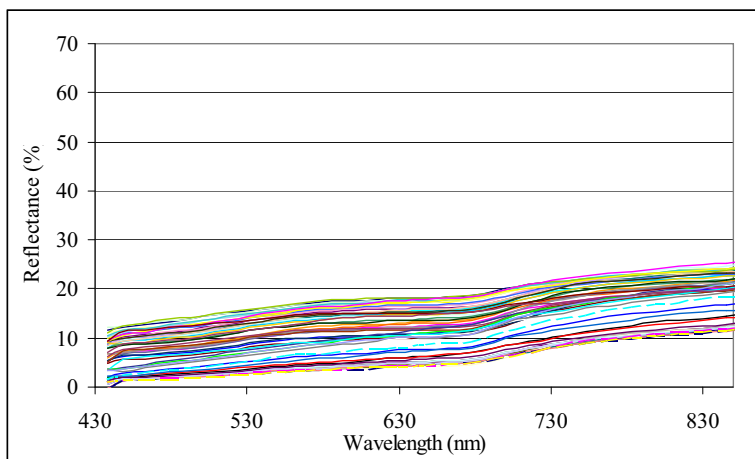


Fig. 3. Spectral signature of soils extracted from airborne Probe-1 imagery.

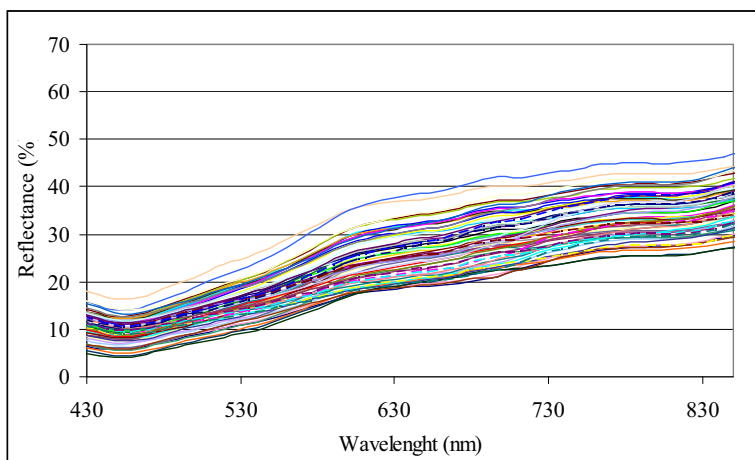


Fig. 4. Spectral signature of soils extracted from Hyperion EO-1 satellite imagery.

#### 4. Results and discussion

For an accurate interpretation of hyperspectral chlorophyll indices, a “true” chlorophyll index value, attributed only to the green vegetation signal and free from any contribution of non-photosynthetic elements, is needed. Theoretically, if only bare soils were considered, with no vegetation, the value of the “ideal” chlorophyll index should be zero regardless of any changes in soil optical properties. Graphically, if a chlorophyll index is computed over bare soils and plotted against the reflectance of the shortest wavelength position used in the index, the clusters of sampling points should then be perfectly superimposed to the theoretical soil line (Huete *et al.*, 1985; Bannari *et al.*, 1996). Unfortunately, chlorophyll indices used to estimate vegetation pigments still show various levels of sensitivity to the effect of soil optical properties.

Index	Required Wavelength Position	Wavelength Position Available From the Hyperion Sensor	Wavelength Position Available From the Probe-1 Sensor
PRI	531 and 550 nm	529.66 and 550.01 nm	537.5 and 552.8 nm
SRPI	430 and 680 nm	428.0 and 682.29 nm	435.7 and 675.7 nm
NDPI	430 and 680 nm	448.47 and 682.50 nm	435.7 and 675.7 nm
CARI	550, 670 and 700 nm	550.22, 672.32 and 702.01 nm	552.8, 675.7 and 705.2 nm
NPCI	430 and 680 nm	448.47 and 682.50 nm	435.7 and 675.7 nm
SIPI	445, 680 and 800 nm	448.47, 682.50 and 803.54 nm	446.2, 675.7 and 797.0 nm
GNDVI	550 and 801 nm	550.22 and 803.54 nm	552.8 and 797.0 nm
PSND <sub>a</sub>	680 and 800 nm	682.54 and 803.54 nm	675.7 and 797.0 nm
PSSR <sub>a</sub>	680 and 800 nm	682.50 and 803.54 nm	675.7 and 797.0 nm
MCARI	550, 670, 700 and 800 nm	550.22, 672.32, 702.01 and 803.54 nm	552.2, 675.7, 705.2 and 797.0 nm
HNDVI	668 and 827 nm	671.02 and 823.65 nm	675.7 and 827.6 nm
CAI	600 and 735 nm	599.79 and 732.07 nm	599.0 and 735.8 nm
TCARI	550, 670 and 700 nm	550.22, 672.32 and 702.01 nm	552.8, 675.7, 705.2 and 797.0 nm
MTCI	681.25, 708.75 and 753.75 nm	682.29, 712.50 and 753.17 nm	675.7, 705.2 and 751.0 nm

Table 3. Available wavelength positions from the Hyperion and Probe-1 sensors for spectral chlorophyll indices calculation.

To evaluate the sensitivity of chlorophyll indices, included in this study, to changes of soil optical properties, the relationship between each of these indices and the shortest wavelength position involved in their formula was analyzed for different bare soils observed at three different scales using a field spectroradiometer, an airborne sensor (Probe-1), and a space-borne sensor (Hyperion EO-1). Hence, while field spectroradiometric measurements provide the wavelength positions needed for each index, spectra extracted from Probe-1 and Hyperion images do not contain all the exact wavelength positions



required for these indices. Thus, wavelengths were selected which most closely match the wavelengths position proposed for the indices investigated (Table 3).

The relationships between chlorophyll indices and their shortest wavelengths, over bare soils, are not unique; they show a considerable scatter caused by changes in soil optical properties. In fact, these indices were designed from leaf or canopy spectra to measure vegetation pigments. To understand this influence, chlorophyll indices selected for this study were plotted against their shortest wavelength position as illustrated in Figure 5. It shows that in addition to having different levels of sensitivity to soil properties variation, indices studied exhibit different behaviour and trends expressed in terms of the distance between index values and the theoretical soil line and the scatter magnitude of their clusters within the scatter-plot.

The first group, characterized by a horizontal trend showing clouds of points generally parallel to the X-axis of the scatter-plot (theoretical soil line), include CARI, MCARI, TCARI, PRI and MTCI indices (Figure 5-A). They have in common the use of wavelengths from the red-edge, red, and green spectral regions except for PRI which uses only wavelengths from the green portion of the solar spectrum. Such wavelengths are known to be the most sensitive to leaf chlorophyll variations and relatively influenced by changes in soil optical properties. This may explain their constant behavior as a function of their shortest wavelength. It can be seen in Figure 5-A that these indices behavior was not affected by the source of data: observed trends are similar, with index values falling basically within the same cloud of points for ground, airborne, and space-borne data. Regarding the sensitivity magnitude to the soil optical properties, indices of this group exhibit the best overall performance in terms of resistance to soil background effects with exception of MTCI which is very sensitive.

The second group consists of indices showing higher sensitivity to soil background at low reflectance levels of the shortest wavelength, which corresponds to the conditions of dark or developed soils. Figure 5-B shows that the indices HNDVI, PSNRa, and PSSRa follow a horizontal trend for the shortest wavelength reflectance values exceeding 20%. They appear to be more responsive to soil optical properties when this reflectance tends to decrease, causing a sudden change of the trend with a steep negative slope for reflectance values of less than 20%. Index values of up to 0.5 and 2.5 occur for PSNRa and HNDVI, and PSSRa, respectively. As shown in Table 1, indices of this group either have the particularity of being a simple ratio (PSSRa) or normalized differences (HNDVI and PSNRa) of red and near-infrared wavelengths. These are examples of traditional vegetation indices which are not adjusted for soil optical effects. As expected in this group, PSSRa is the most sensitive to soil influence because as a simple ratio it does not attenuate the background contribution to the observed signal.

## Thank You for previewing this eBook

You can read the full version of this eBook in different formats:

- HTML (Free /Available to everyone)
- PDF / TXT (Available to V.I.P. members. Free Standard members can access up to 5 PDF/TXT eBooks per month each month)
- Epub & Mobipocket (Exclusive to V.I.P. members)

To download this full book, simply select the format you desire below

